Journal of Manufacturing Processes 68 (2021) 923–931

Contents lists available at ScienceDirect

Journal of Manufacturing Processes

journal homepage: www.elsevier.com/locate/manpro

Evolution and control of deformation mechanisms in micro-grooving of Zr-based metallic glass

Pei Qiu [a], Binbin Meng [a], Shaolin Xu [a,*], Yiming Rong [a], Jiwang Yan [b]

[a] Department of Mechanical and Energy Engineering, Southern University of Science and Technology, Shenzhen, China
[b] Department of Mechanical Engineering, Faculty of Science and Technology, Keio University, Yokohama, Kanagawa, Japan

ARTICLE INFO

Keywords:
Metallic glass
Micro-grooving
Depth of cut
Cutting characteristic
Free volume concentration

ABSTRACT

The evolution of deformation mechanisms with increasing depth of cut (DOC) in micro-grooving of Zr-based metallic glass was deeply investigated in this study for the first time. The micro-grooving characteristics of metallic glass were initially studied by nanoscratch test, which verified that the material removal mode abruptly changes from extrusion mode to cutting mode with increase of DOC. Based on the free-volume theory, a dynamic model coupling stress, temperature and free volume concentration was used to simulate the change of deformation characteristics with DOC. The results showed that the deformation mechanism of metallic glass is closely related to free volume flow, which is significantly affected by average strain rate and free volume flow coefficient in deformation zone and can be tuned with different DOC. Considering that free volume flow is determined by its flow coefficient and concentration, we proposed to control the deformation characteristics of metallic glass in micro-grooving by heat treatment and verified its effectiveness experimentally.

1. Introduction

Metallic glass (also called amorphous alloy) is a kind of metal material with a long-range disordered atom structure obtained by the rapid quenching method. These materials exhibit unique characteristics, such as high strength, high elasticity and excellent corrosion/wear resistance [1]. Based on these characteristics, metallic glass is a suitable nano-moulding material [2–4], while their polycrystalline metal counterparts are restricted by the crystalline grain size [5,6]. Due to the ability to easily produce any desired shape, mechanical micromachining has become the most commonly used technique to obtain complex microstructures on metallic glass [7–9]. Hence, it is very useful to study the deformation characteristics of metallic glass in micron and submicron scales for improving its machining quality.

Due to the absence of grain boundaries and dislocations, the deformation behavior of metallic glass is significantly different from crystal metals [10]. The influence of cutting parameters on machined surface quality, chip morphology and tool wear during metallic glass machining was mainly studied [11–17]. In the cutting parameters, depth of cut (DOC) is one of the most important parameters that affect the deformation characteristics of materials in mechanical machining, thus affecting machining quality. The research on the formation of a shear band of metallic glass showed that there are serration chips composed of the primary shear band and a secondary shear band when DOC is greater than 20 μm [14,15], which is consistent with macro-cutting characteristics [18,19]. Micro-grooving experiments of NiP amorphous alloy coating indicated that the machined grooves' quality is independent of DOC from several to several tens of micrometers [17]. When the DOC is in the submicron scale, the cutting process research of metallic glass usually adopts the method of simulation. Molecular dynamics simulation of chip formation in nanometric cutting of metallic glass showed that there is no visible shear zone ahead of the tool unlike the experimental results in the micron scale [20]. Furthermore, the nano-cutting simulation of Zr50Cu50 metallic glass by molecular dynamics method showed that the removal of the material is mainly by extrusion rather than shearing [21]. Actually, due to these deformation characteristics at the submicron scale, the mirror surface cannot be obtained even when the DOC is set as 0.6 μm [13].

In addition to machining experiments, nanoscratch test is also used to study the effect of DOC on deformation characteristics. In order to study grinding characteristics and wear resistance of metallic glass, nanoscratch tests are carried out by a Berkovich pyramid indenter to explore the deformation and removal mechanism in the grinding and wear process [22–25]. Micro-scratch studies on Fe-based metallic glass

* Corresponding author.
E-mail address: xusl@sustech.edu.cn (S. Xu).

https://doi.org/10.1016/j.jmapro.2021.06.012
Received 15 June 2020; Received in revised form 6 June 2021; Accepted 6 June 2021

and Mg-based metallic glass show that deformation characteristics of metallic glass change with DOC. For example, when the loading force is 75 mN, the scratch in Fe-based metallic glass is very uniform with no visible features at the borders and devoid of any debris. In contrast, the shear band at scratch edge can be observed under 105 mN [22]; With increase of DOC, the wear mechanism of Mg-based BMG changes from rubbing or plowing to cutting [23]. The previous studies have proven that the deformation characteristics of metallic glass are quite different with DOC of micron and submicron scales.

As a key technology in ultra-precision machining of micro/nano-structures, micro-grooving characteristics of metallic glass with different DOC still lack in-depth study, which cannot be explained by the size effect caused by factors like grain size or dislocation density in polycrystalline alloy [26]. The metastable state of metallic glass with an irregular arrangement of atoms makes its plastic deformation mechanism sophisticated in mechanical machining, in which the coupling effect of temperature, stress and free volume changed with time has to be taken into account [11,27,28]. The lack of comprehensive study on mechanical deformation behavior, especially at the micron and submicron scales, restricts the improvement of the surface quality of mechanically machined grooves of metallic glass.

In this paper, micro-grooving of Zr-based metallic glass is carried out to study the influence of DOC on machined surface characteristics in micron and submicron scales. Considering the complex deformation characteristics of metallic glass, a dynamic simulation model based on free volume theory [28–32] is used to analyze the influence of DOC on the coupling effect of stress, temperature and free volume concentration with time in deformation zone. Since the free volume concentration is a key factor affecting the free volume flow and thus plastic deformation ability, it is theoretically possible to control the material removal mode of metallic glass by modulating free volume concentration. Previous studies on the effect of heat treatment on metallic glasses showed that free volume concentration changes along with localized atomic arrangement [33]. Specifically, the annealing treatment can increase the internal topological order of metallic glass, and this more ordered atomic arrangement will reduce the free volume [34]; cryogenic treatment can make the local atomic arrangement of metallic glass more disordered, which will increase the free volume [35,36]. Therefore, in this paper, we propose to control the deformation mechanisms of metallic glass in the micro-grooving process by heat treatment, and its effectiveness is verified by experiments.

2. Experimental study on micro-grooving of metallic glass

2.1. Experimental design

Nanoscratch test with constantly increasing normal load (Progressive load) is used to mimic the influence of DOC on the micro-grooving characteristics of metallic glass, Fig. 1(a) illustrates the experimental equipment. Grooving operations are carried out on an Anton Paar instrument nanoscratch tester, whose normal load can be accurately controlled instantaneously through a closed-loop force feedback system of the equipment with a resolution of 0.01 mN to keep the normal force precisely controlled. It can also measure lateral force and DOC at the same time. The samples of the present study are Zr-based metallic glass ($1 \times 10 \times 10$ mm^3) with nominal composition ZrCuNiAlNbRe and all specimens are mechanically polished to be mirror surfaces with Ra less than 8 nm before grooving experiments.

It is noteworthy that this paper mainly studies the grooving process of metallic glass, so a custom V-shaped diamond tool commonly used in surface structure fabrication was selected. The tool and its profile are shown in Fig. 1(b) and (c), the tool holder is designed with a flat locating surface that can be matched with the flat surface in the tool shank, which is also parallel to the tool rake face. This helps to make the rake face perpendicular to the cutting direction in the micro-grooving. Other experiment parameters and the detailed parameters of the tool are shown in Table 1.

2.2. Analysis of cutting characteristics under different DOC

Micro-grooving of Zr-based metallic glass is analyzed based on experiments under continuously varying DOC, so the linearly increased loading force is used in this study. The micro-grooving characteristics of metallic glass are analyzed from cutting force, groove morphology and elastic recovery.

Fig. 2 shows the variation of lateral force (F_l) and groove depth (P_d) versus normal load (F_n) during the scratch process. When F_n is less than 40 mN, F_l increases slowly from 0 to 20 mN, and P_d increases gradually to 650 nm. When F_n is around 40 mN, F_l and P_d change abruptly, and increase to 75 mN and 3400 nm, respectively. The results of the scratch test under progressive load show that the material removal process changes with the DOC. And there seems to be a critical DOC in the cutting process of Zr-based metallic glass.

A scanning electron microscope (SEM, Zeiss Merlin) was used to observe the groove morphology at different DOC. And to facilitate the comparison of groove morphology before and after the critical DOC, constant load scratch experiments were also carried out with normal forces of 20 mN, 30 mN and 50 mN, respectively. Fig. 3(a) shows the scratch morphology before and after the critical DOC. In Fig. 3(a1), there is a large amount of material pile up on both sides of the groove, while in Fig. 3(a3), a much smoother groove was obtained and the material accumulation along groove edges disappears. Fig. 3(b) shows the morphology of the head and tail of scratch groove at constant loads of 20 mN, 30 mN and 50 mN. When the DOC is less than the critical depth, the deformation of metallic glass tends to extrude and pile up to both sides instead of completely cutting removal. This is the first time to observe the extrusion removal process in micro-grooving of metallic glass by experimental method.

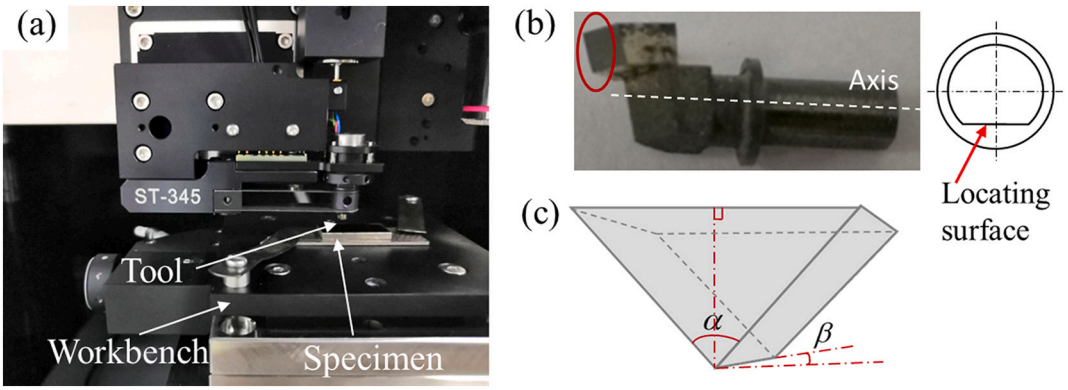

Fig. 1. (a) Nanoscratch tester (b) the V-shaped cutting tool (c) sketch of the tool.

Table 1
Experimental conditions.

Micro-grooving experiments	Progressive load (F_n)	0.1–50 mN
	Load resolution	0.01 mN
	Constant load (F_n)	20, 30, 50 mN
	Scratch length	2000 μm
	Scratch velocity	5000 μm/min
V-shaped tool	Material	Single crystalline diamond
	Rake angle	0°
	Clearance angle (β)	8°
	Nose angle (α)	90°
	Nose radius	Dead-sharp

In order to compare the characteristics of the two removal modes, only two processing conditions with normal forces of 20 mN and 50 mN are selected for comparison. Fig. 4 shows scratch depth and lateral force under constant load. It can be seen that the process is divided into two stages: the initial stage and the stable stage. In the stable stage, the average scratch depth was 415 nm under the normal load of 20 mN, while it was 3495 nm under the normal load of 50 mN. In addition, the residual depth of micro-grooves was measured by a high-resolution confocal laser scanning microscope (CLSM, Keyence vk-x1000) and the results are shown in Fig. 5. Eight different positions are selected to measure the depth of the groove under different loads. When the DOC is 415 nm and 3495 nm, the average residual depth is 268.25 nm and 3322.5 nm, respectively. It can be calculated that the elastic recovery is 35.36% in the extrusion removal stage and only 4.94% in the cutting removal stage. This shows that extrusion removal is mainly elastic-plastic deformation, while the cutting removal process mainly belongs to plastic deformation.

In summary, the micro-grooving experiments show that the DOC seriously affects the cutting characteristics: when the DOC is smaller than the critical depth, Zr-based metallic glass will undergo elastic-plastic deformation, and the material removal method is extrusion

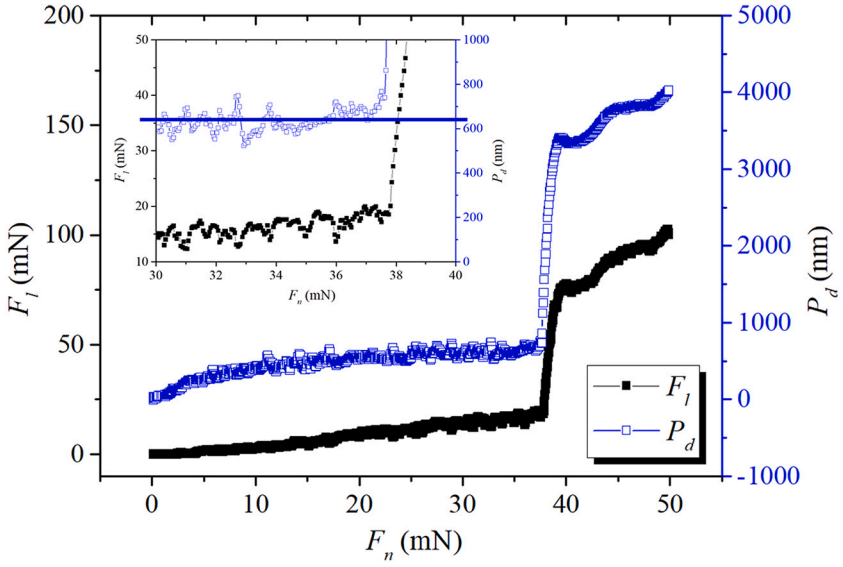

Fig. 2. Plot of lateral force F_l and groove depth P_d against normal load F_n.

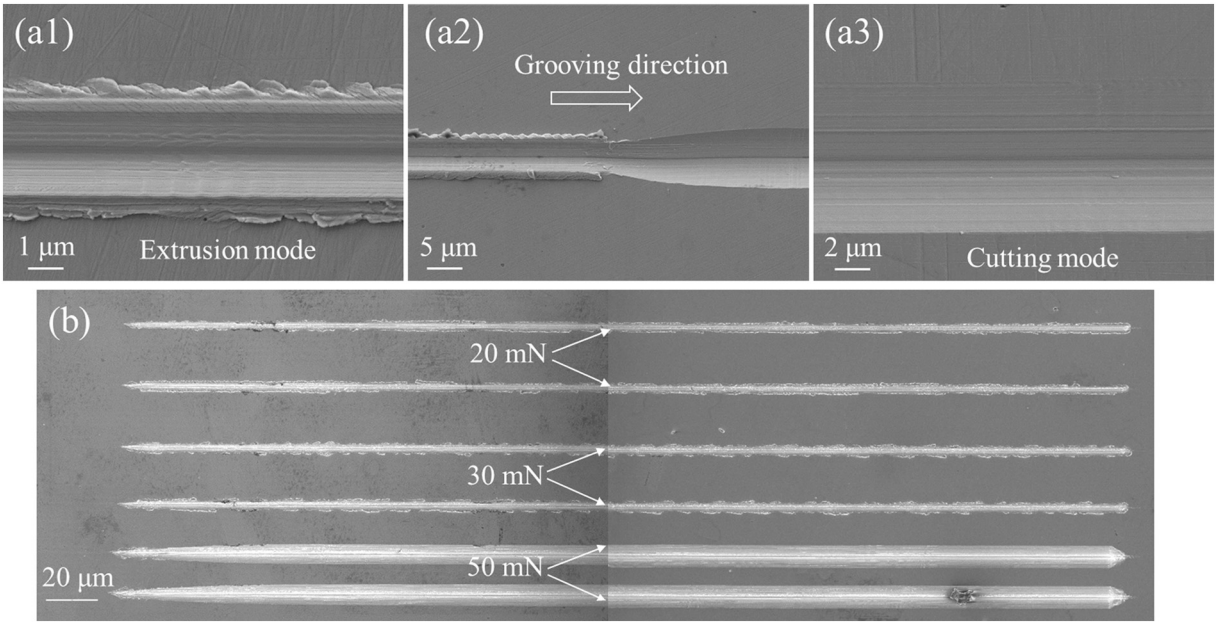

Fig. 3. Groove morphology under (a) progressive normal load (b) different constant load.

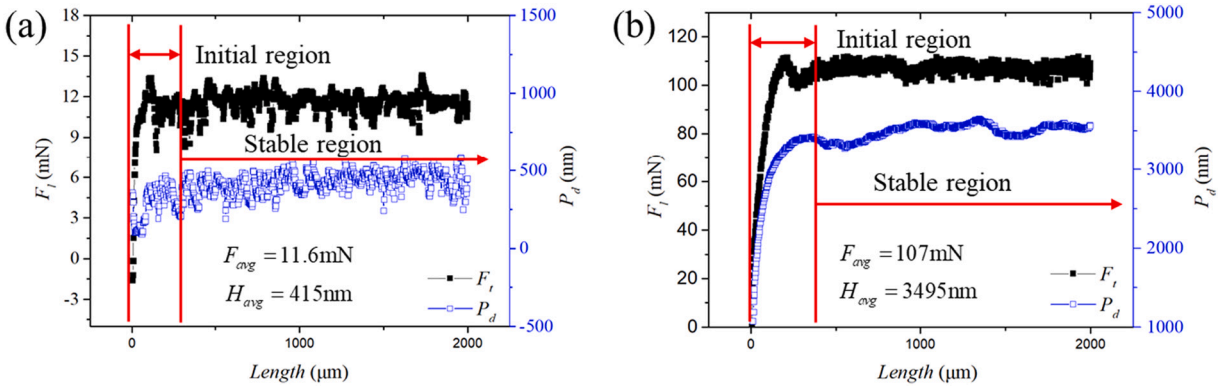

Fig. 4. The cutting force and penetration depth comparison with different normal load. (a) F_n = 20 mN (b) F_n = 50mN.

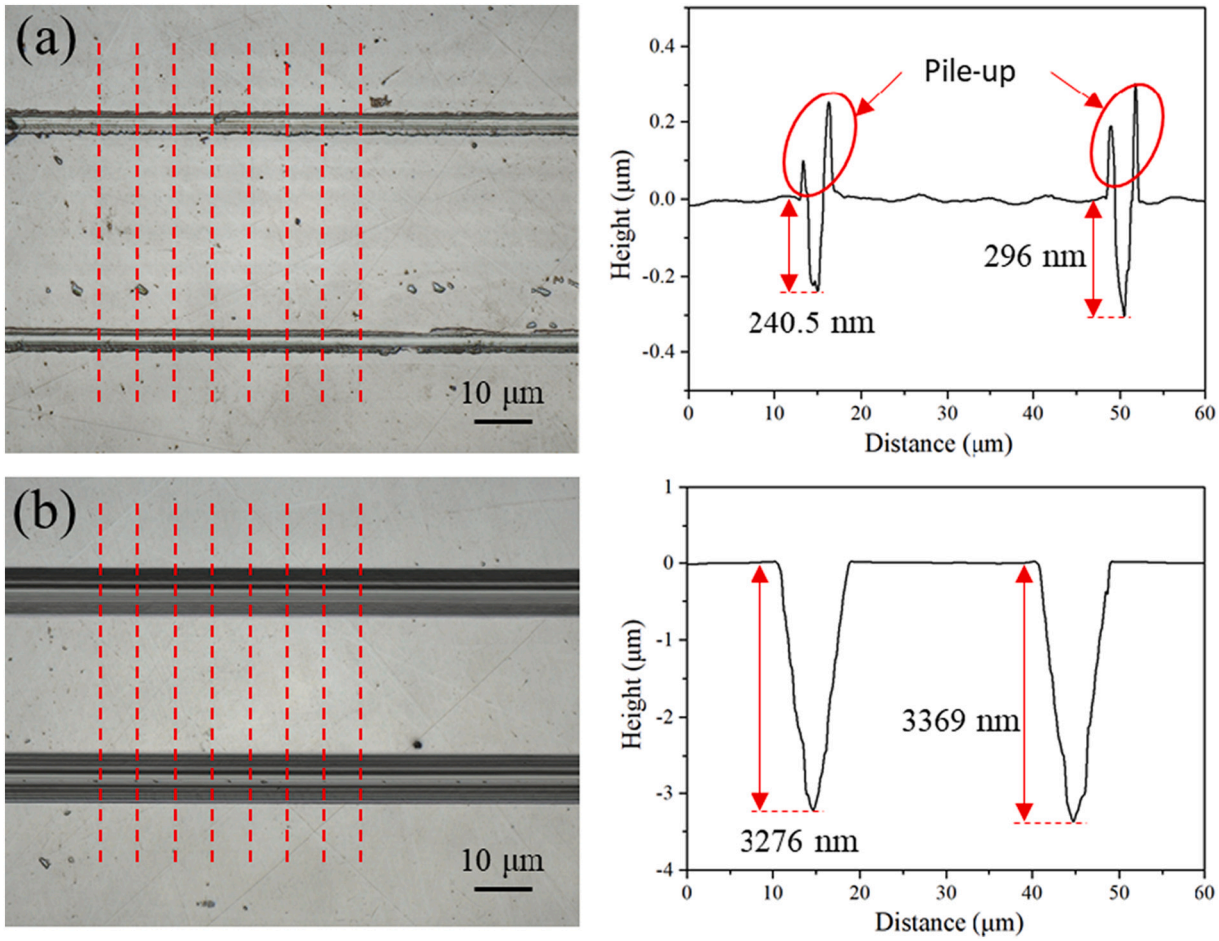

Fig. 5. Residual depths of micro-grooves when (a) F_n = 20 mN (b) F_n = 50 mN.

removal process; otherwise, the material removal process of Zr-based metallic glass is cutting process and it mainly undergoes plastic deformation. It is well known that the plastic deformation mechanism of metallic glass is sophisticated and the coupling effect of temperature, stress and free volume concentration changing with time should be taken into account. Therefore, in the following content, the dynamic model [28–32] based on free volume theory was used to analyze the evolution mechanism of material deformation characteristics caused by DOC.

3. Simulation and analysis of deformation mechanism under different DOC

3.1. The dynamic simulation model

The cutting process of metallic glass involves the changes of stress, temperature and free volume concentration [37]. The free volume will be reproduced or annihilated under the action of stress and temperature, then affecting the stress and temperature dynamically [33,38]. Meanwhile, the free volume will diffuse due to the concentration gradient, and the heat will be transferred out of deformation zone due to the temperature gradient. Hence, stress, temperature and free volume

concentration will change dynamically with time in the material removal process [11,28,31,32].

In the process of machining, when the shear stress exceeds the yield stress of the metallic glass, the plastic flow of the material in deformation zone will dissipate the accumulated strain energy, which leads to the decline of the shear stress. Therefore, the variation of shear stress with time is related to the difference between average strain rate $\dot{\gamma}_{avg}$ and plastic strain rate $\dot{\gamma}^p$, as shown in Eq. (1).

$$\frac{\mathrm{d}\tau}{\mathrm{d}t} = \Lambda\left(\dot{\gamma}_{avg} - \dot{\gamma}^p\right) \tag{1}$$

where $\Lambda = El h \sin^2\phi/\Gamma d^2$, E is Young's modulus, l is the length of tool contact with the chips, h is the thickness of primary shear zone (PSZ), ϕ is the shear angle, Γ is the coefficient between the friction force and normal force, d is the DOC; $\dot{\gamma}_{avg} = V_s/h$ is the average strain rate applied on the PSZ, V_s is the shear velocity.

The plastic strain rate $\dot{\gamma}^p$ is determined by the atomic displacement per unit time, and whether the atom can jump depends on the activation energy ΔG_m applied by the external force. Only if the activation energy is greater than the potential barrier, the atomic displacement occurs. So the plastic strain rate can be expressed by the fraction of potential-jump sites times the net number of forwarding jumps at each site per second, as the following equation

$$\dot{\gamma}^p = 2fexp\left(-\frac{1}{\xi}\right)sinh\left[\frac{\tau\Omega}{2k_BT}\right]exp\left[-\frac{\Delta G_m}{k_BT}\right] \tag{2}$$

where f is the frequency of atomic vibration, ξ is the free volume concentration, Ω is the atomic volume, k_B is the Boltzmann constant, T is the absolute temperature, and ΔG_m is the activation energy.

When plastic deformation occurs in metallic glass, its atomic arrangement in deformation zone will be more disordered and the free volume will increase. This process is described by the net production rate of free volume $g(\tau,\xi,T)$. However, nearby atoms will jump to the vacancy when a free volume occurs to keep the local lowest free energy. The possibility of this kind of atom displacement in all directions is only related to the gradient of free volume concentration. Thus, the reduction of free volume can be described as a diffusion process, which results in a lower free volume concentration in deformation zone. The time differential of free volume concentration can be expressed as:

$$\frac{\mathrm{d}\xi}{\mathrm{d}t} = \eta(\xi_0 - \xi) + g(\tau,\xi,T) \tag{3}$$

where $\eta = (V_f + 4D/h)/h$ is the free-volume flow coefficient with the diffusion coefficient D of ξ, ξ_0 is the free volume concentration outside the PSZ, $g(\tau,\xi,T)$ is the net generation rate function of ξ refer to [27,32], V_f is the chip velocity.

The plastic deformation of metallic glass will increase its strain energy and the release of strain energy will increase the temperature of deformation zone. On the other hand, the temperature gradient between the deformed zone and the undeformed zone will lead to the heat conduction process. So the temperature of deformation zone is given by

$$\frac{\mathrm{d}T}{\mathrm{d}t} = \vartheta(T_0 - T) + A\tau\dot{\gamma}^p \tag{4}$$

where $\vartheta = (V_f + 4\kappa/h)/h$ is the heat flow coefficient with the thermal diffusivity κ, T_0 is the absolute temperature outside the PSZ, $A = \beta_{TQ}/\rho C_v$ is a constant related to the Taylor–Quinney coefficient β_{TQ} with the density ρ and the specific heat C_v.

To reduce the calculation error caused by the magnitude difference of each parameter, the parameter is usually normalized. Select dimensionless parameter as $\widehat{T} = T/T_0$, $\widehat{t} = t/t_0$ with $t_0 = f^{-1}\,exp\,(\Delta G_m/k_BT_0)$, $\widehat{\tau} = \tau/\tau_0$ with $\tau_0 = 2k_BT_0/\Omega$, then dropping the hats, we have the dimensionless forms of governing Eqs. (5)–(8):

$$\frac{\mathrm{d}\tau}{\mathrm{d}t} = \Lambda'\left(\dot{\gamma}_{avg}{}' - \dot{\gamma}^p\right) \tag{5}$$

$$\dot{\gamma}^p = 2exp\left[\frac{\Delta G_m}{k_BT_0}\left(1-\frac{1}{T}\right)\right]exp\left(-\frac{1}{\xi}\right)sinh\left[\frac{\tau}{T}\right] \tag{6}$$

$$\frac{\mathrm{d}\xi}{\mathrm{d}t} = \eta'(\xi_0 - \xi) + \frac{1}{\varphi}exp\left[\frac{\Delta G_m}{k_BT_0}\left(1-\frac{1}{T}\right)\right]exp\left(-\frac{1}{\xi}\right)\times\left\{\frac{T}{\Phi\xi}\left[cosh\left(\frac{\tau}{T}\right)-1\right]-\frac{1}{n_D}\right\} \tag{7}$$

$$\frac{\mathrm{d}T}{\mathrm{d}t} = \vartheta'(1-T) + A\frac{\tau_0}{T_0}\tau\dot{\gamma}^p \tag{8}$$

where $\Lambda' = \Lambda/\tau_0$, φ is a geometrical factor [31]. $\Phi = \frac{2}{3}\frac{1+\nu}{1-\nu}\frac{v^*}{\Omega}\frac{G}{\tau_0}$ with Poisson ratio ν, the critical volume v^* of the effective hard-sphere size of atom, and the shear modulus G, n_D is the number of diffusive jumps necessary to annihilate a free volume equal to v^*, $\eta' = \eta\cdot t_0$, $\vartheta' = \vartheta\cdot t_0$, $\dot{\gamma}_{avg}{}' = \dot{\gamma}_{avg}\cdot t_0$.

In Section 2, it is found that the cutting characteristics are significantly different before and after the critical DOC. To explain this phenomenon, DOC = 10 μm and DOC = 0.1 μm are selected in the numerical calculation. The DOC with two orders of magnitude difference can enlarge the difference between the extrusion removal process and the cutting removal process. It can also make up for the calculation accuracy problem caused by the inaccuracy of some parameters in the formula. The values of those variables used in the simulation are shown in Table 2, other parameters are referred to reference [11].

3.2. The influence of DOC on the deformation characteristics

Fig. 6 shows that in the cutting removal process, periodic vibration occurs in stress, free volume concentration and temperature. First of all, plastic deformation occurs in the primary shear zone under the action of stress, which makes the free volume in PSZ accumulate to form a shear band, and the formation of shear band will reduce shear stress and thus reduce the continuous accumulation of free volume. When the shear band is discharged, another part of the materials entering the main shear zone will repeat the above formation and discharge process. Because the deformation of the material is accompanied by the change of temperature, the periodic fluctuation of stress, temperature and free volume concentration is formed. According to the vibration period and cutting speed, it can be calculated that the vibration interval is about 100 nm, which is equal to the space interval of the secondary shear band [29,39].

In the extrusion removal process, the stress, free volume concentration and temperature quickly reach a stable state, indicating that there is no shear band formation and discharge process, which is significantly different from the macron cutting or micron cutting [12,14,15,18,19]. Because the free volume flow coefficient increases significantly with the decrease of the DOC, the free volume is not easy to accumulate, and the formation of the shear band is more difficult; while the average strain

Table 2
Dimensionless parameters for simulation.

DOC (μm)	10	0.1
$\dot{\gamma}_{avg}'$	0.001	0.1
η'	0.04	4
ϑ'	40	400,000
ξ_0	0.045/0.05/0.055	0.045/0.05/0.055

rate increases, the deformation ability is improved, so there is a large amount of material pile up on both sides of the groove. Therefore, there is no fluctuation in the extrusion removal process without shear band formation.

Through the simulation analysis, it can be concluded that the deformation mechanism of metallic glass is closely related to free volume flow, which is determined by the free volume flow coefficient and concentration. The DOC essentially affects the average strain rate and free volume flow coefficient of metallic glass in deformation zone, causing that the material removal process shows two modes: extrusion mode and cutting mode.

4. Control of material removal mode of metallic glass

Since free volume concentration is a key factor affecting the properties of metallic glass, the initial free volume concentration is adjusted to change the cutting characteristics of metallic glass at different DOC. Firstly, the change rule of stress, free volume concentration and temperature under different initial free volume concentrations is analyzed by simulation, then the influence of initial free volume concentration on cutting characteristics is analyzed by experiment to verify the feasibility of the control method.

4.1. Simulation analysis of the control by adjusting the free volume concentration

As shown in Fig. 7, under the same DOC, if the initial free volume concentration ξ_0 of the workpiece increases or decreases by 0.005, the vibration disappears and intensifies respectively. When the free volume concentration increases, the volume of the deformation units is relatively large, and only a small external force is needed to remove the material; when the free volume concentration decreases, the deformation units need larger shear stress and a longer accumulation time to form a shear band, so the amplitude and the vibration period increase.

Through the comparison of three sets of simulation results, it is considered that changing the initial free volume concentration can change the critical depth of extrusion deformation, and can be used to control the removal mode from extrusion to cutting. For example, when the ξ_0 increases to 0.055, even if DOC is 10 μm, it may show the characteristics of extrusion removal; when the ξ_0 decreases to 0.045, it may be represented as cutting removal mode even if the DOC is 0.1 μm.

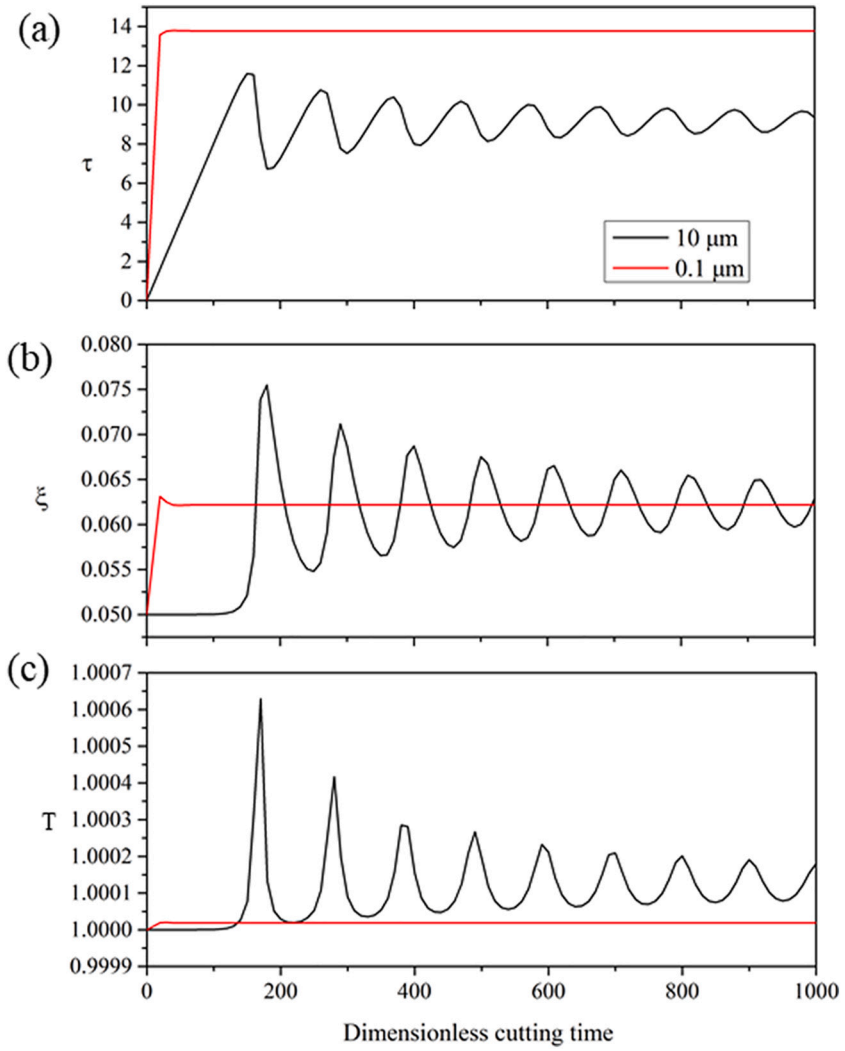

Fig. 6. Shear stress, free volume concentration, and temperature vs. cutting time from simulations of Eqs. (5)–(8) with DOC = 10 μm and DOC = 0.1 μm, $\xi_0 = 0.05$.

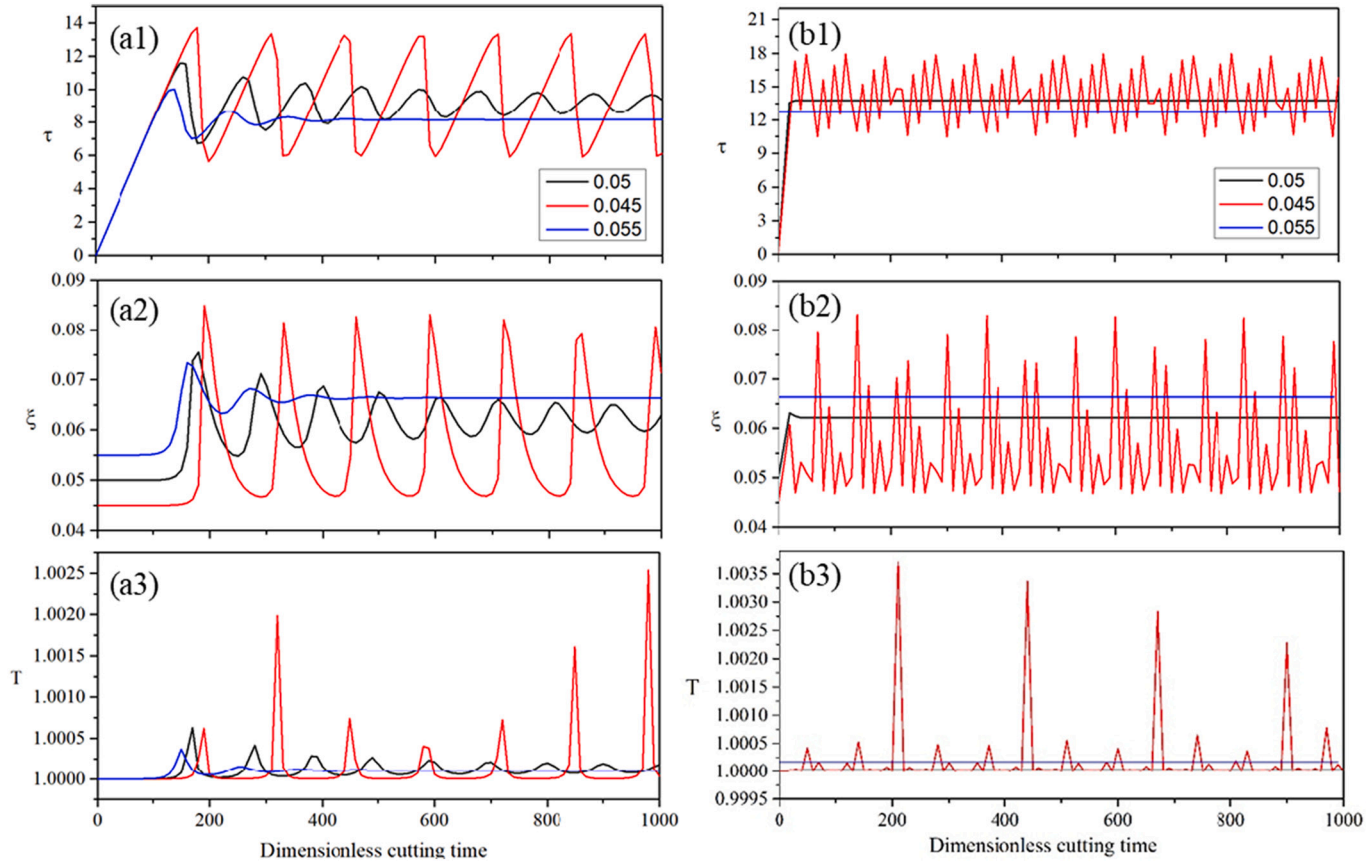

Fig. 7. Shear stress, free volume concentration, and temperature vs. cutting time from simulations of Eqs. (5)–(8) with $\xi_0 = 0.05, 0.045, 0.055$ (a) $d = 10$ μm, (b) $d = 0.1$ μm.

4.2. Experimental verification of the control method of material removal mode by adjusting the free volume concentration

The deformation or heat treatment can change the free volume concentration of metallic glass [40,41]. However, it is difficult to control free volume concentration caused by deformation, and pre-deformation is not convenient for machining, so two kinds of heat treatment methods are conducted to obtain two kinds of initial free volume concentration: as-cast specimens were heated to 0.8 Tg (628 K) by 3 K/min and cooled slowly to room temperature after holding for 2 h to obtain a structural-relaxation sample; as-cast specimens were frozen in liquid nitrogen for 2 h to obtain a rejuvenated sample. Meanwhile, the amorphous structures of these metallic glasses under different conditions were ascertained by X-ray diffraction (Rigaku Smartlab, 9KW) as shown in Fig. 8.

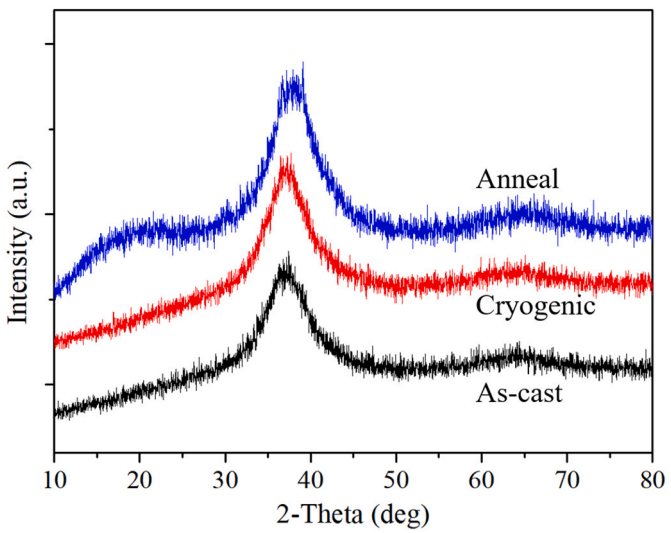

Fig. 8. XRD pattern of samples under different heat treatment.

Fig. 9(a, b) shows the curves of lateral force (F_l) and groove depth (P_d) versus normal load (F_n) of materials with different heat treatments under progressive load. F_l and P_d also change abruptly with F_n increases, which is consistent with the previous result, but the critical depth change. Fig. 9(c) shows the results of critical depth measured by three groups of experiments under various initial states. It demonstrates that the critical depth of annealed specimen (about 478 nm) is slightly smaller than that of as-cast material (about 648 nm), while the critical depth of rejuvenation metallic glass (about 924 nm) is larger than that of as-cast and relaxed material.

The critical depth of deformation transition changes with different initial free volume concentrations. These experimental results are consistent with the numerical results, which show that heat treatment can control the material removal mechanism.

5. Conclusions

In this paper, the effects of DOC on the micro-grooving characteristics of metallic glass are studied systematically. The following conclusions can be drawn:

(1) There is a critical transition DOC in the micro-grooving of metallic glass, through which the material removal mode changes from extrusion mode to cutting mode. In the extrusion removal mode, material piles up on both sides of grooves, while in the cutting removal mode, smooth grooves can be obtained.

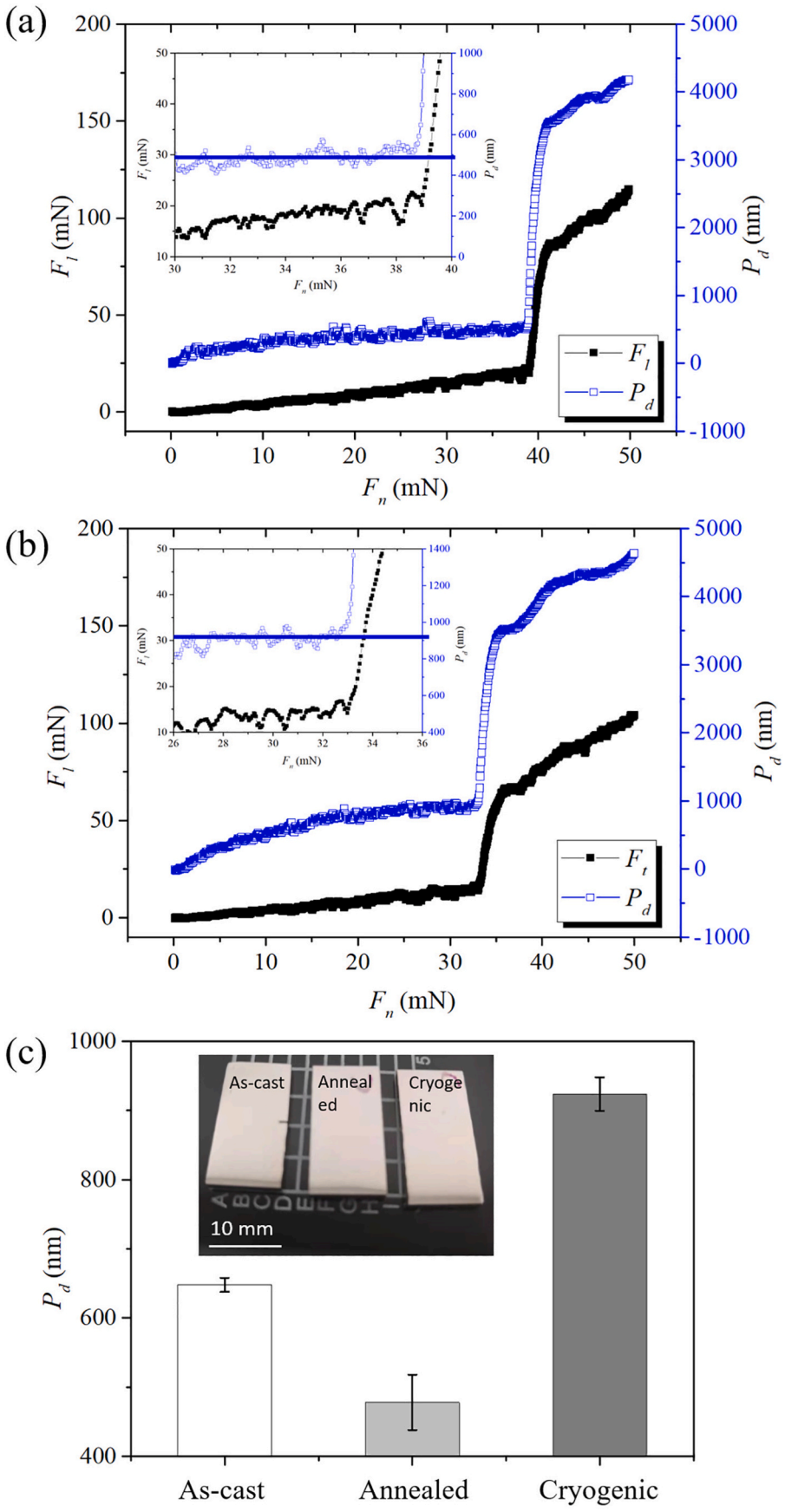

Fig. 9. Variation of scratch depth and lateral force with loading force (a) annealed sample (b) cryogenic sample (c) Critical DOC of different samples.

(2) The change of DOC mainly affects the average strain rate and the free volume flow coefficient of materials in deformation zone, thus changing the removal characteristics of metallic glass. The increase of free volume flow coefficient due to the decrease of DOC makes it difficult to form a shear band. On the other hand, the plasticity of metallic glass increases as the average strain rate increases, which makes the plastic removal process more stable.
(3) Heat treatment can be used to control the free volume concentration of metallic glass and thus modulate its plastic deformation ability. So the critical transition DOC can be adjusted by annealing and cryogenic treatment.

Declaration of competing interest

The authors declare that they have no known competing financial interests or personal relationships that could have appeared to influence the work reported in this paper.

Acknowledgments

This work was financially supported by the Guangdong Provincial University Science and Technology Program (Grant No. 2020KTSCX119) and the Shenzhen Science and Technology Programs (Grant No. GJHZ20190820151801786, KQTD20170810110250357).

References

[1] Wang WH, Dong C, Shek CH. Bulk metallic glasses. Mater Sci Eng R 2004;44:45–89. https://doi.org/10.1126/science.1158864.
[2] Kumar G, Tang HX, Schroers J. Nanomoulding with amorphous metals. Nature 2009;457:868–72. https://doi.org/10.1038/nature07718.
[3] Sakurai J, Abe M, Ando M, Aono Y, Hata S. Searching for noble Ni-Nb-Zr thin film amorphous alloys for optical glass device molding die materials. Precis Eng 2011;35:537–46. https://doi.org/10.1016/j.precisioneng.2011.05.004.
[4] Sakurai J, Hata S, Yamuchi R, Abe M, Shimokohbe A. Searching for Pt-Zr-Ni thin film amorphous alloys for optical glass lenses molding materials. Precis Eng 2010;34:431–9. https://doi.org/10.1016/j.precisioneng.2009.12.007.
[5] Bardt JA, Bourne GR, Schmitz TL, Ziegert JC, Sawyer WG. Micromolding three-dimensional amorphous metal structures. J Mater Res 2007;22:339–43. https://doi.org/10.1557/jmr.2007.0035.
[6] Schroers J, Pham Q, Desai A. Thermoplastic forming of bulk metallic glass—applications for MEMS and microstructure fabrication. J Microelectromech Syst 2007;16:240–7. https://doi.org/10.1109/JMEMS.0007.892889.
[7] Cardoso P, Davim JP. A brief review on micromachining of materials. Rev Adv Mater Sci 2012;30:98–102. https://doi.org/10.1186/1556-276X-7-96.
[8] Lauro CH, Brandăcz LC, Panzera TH, Davim JP. Surface integrity in the micromachining: a review. Rev Adv Mater Sci 2015;40:227–34.
[9] Chavoshi SZ, Goel S, Morantz P. Current trends and future of sequential micro-machining processes on a single machine tool. Mater Des 2017;127:37–53. https://doi.org/10.1016/j.matdes.2017.04.057.
[10] Shen Y, Li Y, Chen C, Tsai HL. 3D printing of large, complex metallic glass structures. Mater Des 2017;117:213–22. https://doi.org/10.1016/j.matdes.2016.12.087.
[11] Jiang MQ, Dai LH. Formation mechanism of lamellar chips during machining of bulk metallic glass. Acta Mater 2009;57:2730–8. https://doi.org/10.1016/j.actamat.2009.02.031.
[12] Han DX, Wang G, Li J, Chan KC, To S, Wu FF, et al. Cutting characteristics of Zr-based bulk metallic glass. J Mater Sci Technol 2015;31:153–8. https://doi.org/10.1016/j.jmst.2014.11.010.
[13] Chen X, Xiao J, Zhu Y, Tian R, Shu X, Xu J. Micro-machinability of bulk metallic glass in ultra-precision cutting. Mater Des 2017;136:1–12. https://doi.org/10.1016/j.matdes.2017.09.049.
[14] Dhale K, Banerjee N, Singh RK, Outeiro JC. Investigation on chip formation and surface morphology in orthogonal machining of Zr-based bulk metallic glass. Manuf Lett 2019;19:25–8. https://doi.org/10.1016/j.mfglet.2019.01.002.
[15] Ding F, Wang C, Zhang T, Zheng L, Zhu X, Li W, et al. Investigation on chip deformation behaviors of Zr-based bulk metallic glass during machining. J Mater Process Technol 2020;276:116404. https://doi.org/10.1016/j.jmatprotec.2019.116404.
[16] Xiong J, Wang H, Zhang G, Chen Y, Ma J, Mo R. Machinability and surface generation of Pd40Ni10Cu30P20 bulk metallic glass in single-point diamond turning. Micromachines 2020:11. https://doi.org/10.3390/mi11010004.
[17] Kobayashi R, Xu S, Shimada K, Mizutani M, Kuriyagawa T. Defining the effects of cutting parameters on burr formation and minimization in ultra-precision grooving of amorphous alloy. Precis Eng 2017;49:115–21. https://doi.org/10.1016/j.precisioneng.2017.01.018.
[18] Bakkal M, Shih AJ, Scattergood RO, Liu CT. Machining of a Zr-Ti-Al-Cu-Ni metallic glass. Scr Mater 2004;50:583–8. https://doi.org/10.1016/j.scriptamat.2003.11.052.
[19] Bakkal M, Shih AJ, Scattergood RO. Chip formation, cutting forces, and tool wear in turning of Zr-based bulk metallic glass. Int J Mach Tool Manuf 2004;44:915–25. https://doi.org/10.1016/j.ijmachtools.2004.02.002.
[20] Zhao Y, Zhang Y, Liu RP. MD simulation of chip formation in nanometric cutting of metallic glass. Adv Mat Res 2012;476–478:434–7. https://doi.org/10.4028/www.scientific.net/AMR.476-478.434.
[21] Zhu P, Fang F. On the mechanism of material removal in nanometric cutting of metallic glass. Appl Phys A Mater Sci Process 2014;116:605–10. https://doi.org/10.1007/s00339-013-8189-y.
[22] Michler J, Rabe R, Bucaille JL, Moser B, Schwaller P, Breguet JM. Investigation of wear mechanisms through in situ observation during microscratching inside the scanning electron microscope. Wear 2005;259:18–26. https://doi.org/10.1016/j.wear.2005.02.111.
[23] Pan CT, Wu TT, Liu CF, Su CY, Wang WJ, Huang JC. Study of scratching Mg-based BMG using nanoindenter with Berkovich probe. Mater Sci Eng A 2010;527:2342–9. https://doi.org/10.1016/j.msea.2009.11.070.
[24] Rahaman ML, Zhang LC, Ruan HH. Understanding the friction and wear mechanisms of bulk metallic glass under contact sliding. Wear 2013;304:43–8. https://doi.org/10.1016/j.wear.2013.04.022.
[25] Ma MZ, Zong HT, Wang HY, Zhang WG, Song AJ, Liang SX, et al. Indentation and friction of Zr-based bulk metallic glasses on nano-scale. Mater Lett 2008;62:4348–50. https://doi.org/10.1016/j.matlet.2008.07.019.
[26] Davoudi KM, Vlassak JJ. Dislocation evolution during plastic deformation: equations vs. discrete dislocation dynamics study. J Appl Phys 2018:123. https://doi.org/10.1063/1.5013213.
[27] Steif PS, Spaepen F, Hutchinson JW. Strain localization in amorphous metals. Acta Metall 1982;30:447–55. https://doi.org/10.1016/0001-6160(82)90225-5.
[28] Argon AS. Plastic deformation in metallic glasses. Acta Metall 1979;27:47–58. https://doi.org/10.1016/0001-6160(79)90055-5.
[29] Zhang Y, Greer AL. Thickness of shear bands in metallic glasses. Appl Phys Lett 2006:89. https://doi.org/10.1063/1.2336598.
[30] Cohen MH, Turnbull D. Molecular transport in liquids and glasses. J Chem Phys 1959;31:1164–9. https://doi.org/10.1063/1.1730566.
[31] Spaepent F. A microscopic mechanism for steady state inhomogeneous flow in metallic glasses. Acta Metall 1977;25:9.
[32] Timothy JB, Matthew AD. Nonlinear dynamics model for chip segmentation in machining. Phys Rev Lett 1997;79:447–50. https://doi.org/10.1103/PhysRevLett.79.447.
[33] Wakeda M, Saida J, Li J, Ogata S. Controlled rejuvenation of amorphous metals with thermal processing. Sci Rep 2015:5. https://doi.org/10.1038/srep10545.
[34] Meng F, Tsuchiya K, Seiichiro I, Yokoyama Y. Reversible transition of deformation mode by structural rejuvenation and relaxation in bulk metallic glass. Appl Phys Lett 2012;101:1–4. https://doi.org/10.1063/1.4753998.
[35] Ketov SV, Sun YH, Nachum S, Lu Z, Checchi A, Beraldin AR, et al. Rejuvenation of metallic glasses by non-affine thermal strain. Nature 2015;524:200–3. https://doi.org/10.1038/nature14674.
[36] Guo W, Yamada R, Saida J. Rejuvenation and plasticization of metallic glass by deep cryogenic cycling treatment. Intermetallics 2018;93:141–7. https://doi.org/10.1016/j.intermet.2017.11.015.
[37] Qiao JC, Wang YJ, Zhao LZ, Dai LH, Crespo D, Pelletier JM, et al. Transition from stress-driven to thermally activated stress relaxation in metallic glasses. Phys Rev B 2016;94:1–9. https://doi.org/10.1103/PhysRevB.94.104203.
[38] Nekouie V, Doak S, Roy A, Kühn U, Silberschmidt VV. Experimental studies of shear bands in Zr-Cu metallic glass. J Non Cryst Solids 2018;484:40–8. https://doi.org/10.1016/j.jnoncrysol.2018.01.009.
[39] Liu C, Roddatis V, Kenesei P, Maaß R. Shear-band thickness and shear-band cavities in a Zr-based metallic glass. Acta Mater 2017;140:206–16. https://doi.org/10.1016/j.actamat.2017.08.032.
[40] Pan J, Wang YX, Guo Q, Zhang D, Greer AL, Li Y. Extreme rejuvenation and softening in a bulk metallic glass. Nat Commun 2018:9. https://doi.org/10.1038/s41467-018-02943-4.
[41] Pan J, Chen Q, Liu L, Li Y. Softening and dilatation in a single shear band. Acta Mater 2011;59:5146–58. https://doi.org/10.1016/j.actamat.2011.04.047.